

Effect of distribution shape of porosity on the free vibration of FGM plates

Lazreg Hadji¹, Vagelis Plevris² and George Papazafeiropoulos³

¹ Ibn Khaldoun University of Tiaret, Civil Engineering Department, Tiaret, Algeria,
lazreg.hadji@univ-tiaret.dz

² Qatar University, Department of Civil and Environmental Engineering, Doha, Qatar,
vplevris@qu.edu.qa

³ School of Civil Engineering, National Technical University of Athens, Athens, Greece,
gpapazafeiropoulos@yahoo.gr

Abstract. The study investigates the application of trigonometric shear deformation plate theory for the free vibration analysis of functionally graded (FG) plates. The theory takes into account the presence of porosities that can be found in FG materials during their manufacturing process. Four different types of porosity distributions are considered in the analysis of FG plates. The equations of motion are derived using Hamilton's principle, and the governing equations are solved using the Navier procedure. Numerical examples are provided to examine the influence of porosity parameters, porosity types, and geometry parameters on the free vibration characteristics of FG plates. The results reveal that the distribution of porosity significantly affects the mechanical properties of functionally graded plates, particularly in terms of frequency.

Keywords: Free vibration, Functionally graded materials, Porosity, Hamilton's principle.

1 Introduction

The field of materials engineering has experienced significant progress in recent times. One of the particularly fascinating and innovative advancements is the introduction of functionally graded materials (FGMs). Functionally graded materials represent a departure from traditional material design and have garnered considerable interest because of their distinct and adaptable properties. These materials demonstrate a seamless and continuous variation in their thermo-mechanical characteristics, differentiating them from conventional homogeneous materials.

FGMs represent a remarkable achievement in the field of engineering and science, as they offer solutions to complex challenges encountered across a diverse range of industries, including aerospace and biomedical applications. The concept of FGMs was initially introduced by Niknam et al. [1], and it has since paved the way for

exciting developments in materials science and engineering. The underlying principle behind functionally graded materials involves the intentional design of a material that possesses customized properties that seamlessly transition from one end to another [2]. In contrast to traditional materials with uniform properties, FGMs display a gradient, wherein specific characteristics such as mechanical strength, thermal conductivity, or chemical composition gradually vary in a predetermined direction. This distinctive attribute holds immense potential for transforming the design and performance of numerous components and systems.

The applications of functionally graded materials have a wide range of uses. In the aerospace field, they can enhance the performance and durability of critical components, such as turbine blades and heat shields. In biomedical engineering, FGMs can be customized to match the mechanical properties of human tissues, resulting in improved implants and prosthetics. These materials also show promise in energy storage, electronic devices, and the field of architecture, where they can optimize heat distribution and ensure structural integrity. Additionally, given the widespread use of plates in various sectors, such as civil engineering, marine energy conversion, and aerospace engineering [3], it is essential to study their dynamic behavior, particularly in terms of free vibration.

Furthermore, it should be noted that micro voids or porosities may arise within the materials during the sintering phase of FGM fabrication. This is primarily due to the significant difference in solidification temperatures between the various constituents of the material [4]. In their study, Wattanasakulpong et al. [5] discussed the occurrence of porosities in FGM samples fabricated using a multistep sequential infiltration technique. Therefore, it is crucial to consider the impact of porosity when designing FGM structures that are subjected to dynamic loadings. Recently, Wattanasakulpong and Ungbhakorn [6] conducted a study on linear and nonlinear vibration problems of elastically end-restrained FG beams containing porosities. In the studies of Hadji et al. [7, 8] the free vibration of porous functionally graded beams was investigated. In the first paper [7], a higher-order shear deformation model was used and the authors examined the impact of porosity and volume fraction index, different micromechanical models, mode numbers, and geometry on the bending and natural frequencies of FG beams. The other study [8] employed the hyperbolic shear deformation theory without shear correction factors to derive the equations of motion by applying Hamilton's principle. The main objective of the work was to investigate how the distribution of voids affects the free vibration characteristics of FGM beams by utilizing an advanced shear deformation model.

To the best of the authors' knowledge, there is currently no available research that employs the shear and normal deformation theory to comprehensively investigate the bending, vibration, and buckling of FG plates with porosities. These complex problems have not been thoroughly examined, indicating the need for further investigation. Furthermore, there is limited research available that employs the shear deformation theory to investigate the effect of porosity distribution shape on the free vibration of FGM plates. These intricate problems have not been adequately examined, emphasizing the necessity for further research.

This research study presents an investigation into the free vibration response of porous FG plates. The research utilizes a trigonometric shear deformation plate theory to analyze the behavior of these plates. The material properties and porosity distribution of the plates vary along the thickness direction as dictated by the chosen distribution pattern. The governing equations are derived from Hamilton's principle. An analytical solution is provided for the free vibration analysis of porous FG plates. The study also examines and discusses the impact of the porosity distribution pattern and plate geometrical parameters, such as aspect ratio, on the natural frequencies.

2 Functionally graded plates with porosities

A schematic of an FG plate made of two material phases, such as metal and ceramic, is shown in Fig. 1. The material properties of FG plates continuously vary through the thickness of the plate according to power-law form as [9]:

$$P(z) = (P_t - P_b) \left(\frac{z}{h} + \frac{1}{2} \right)^k + P_b, \quad (1)$$

where P_t and P_b denote values of the material properties at the top and bottom of the plate, respectively, and k is the power-law exponent. According to this distribution, the bottom surface (at $z = -h/2$) of the functionally graded plate is pure metal, whereas the top surface (at $z = h/2$) is pure ceramic, and for different values of k , one can obtain different volume fractions of metal.

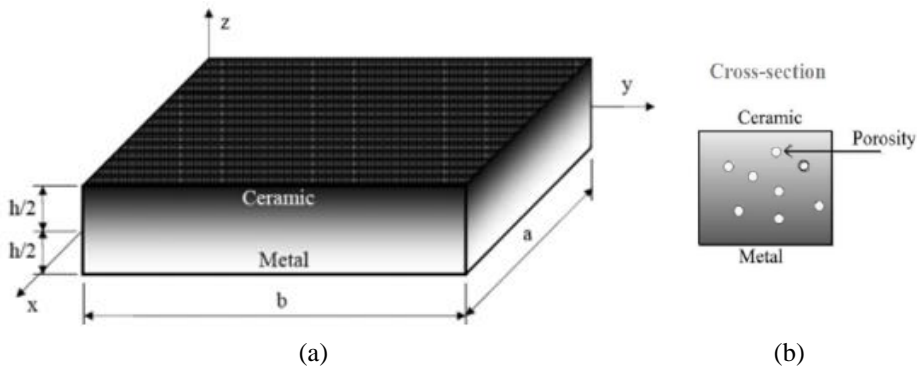






Fig. 1. Geometry of rectangular FG plate and coordinates: (a) 3D view, (b) Cross section.

In the case of a porous FG plate, the rule of mixture must be modified. For even and uneven types of distribution shape of porosity, the modified rule of mixture becomes as shown in Eqs (2), (3), (4) and (5) for the Uniform, X-shape, O-shape and V-shape distribution, respectively [10]:

Uniform 
$$P(z) = (P_t - P_b) \left(\frac{z}{h} + \frac{1}{2} \right)^k + P_b - \frac{\beta}{2} (P_t + P_b) \quad (2)$$

X-shape 
$$P(z) = (P_t - P_b) \left(\frac{z}{h} + \frac{1}{2} \right)^k + P_b - \frac{\beta}{2} (P_t + P_b) \left(2 \frac{z}{h} \right) \quad (3)$$

O-shape 
$$P(z) = (P_t - P_b) \left(\frac{z}{h} + \frac{1}{2} \right)^k + P_b - \frac{\beta}{2} (P_t + P_b) \left(1 - 2 \frac{|z|}{h} \right) \quad (4)$$

V-shape 
$$P(z) = (P_t - P_b) \left(\frac{z}{h} + \frac{1}{2} \right)^k + P_b - \frac{\beta}{2} (P_t + P_b) \left(\frac{1}{2} + \frac{z}{h} \right), \quad (5)$$

where $\beta < 0$ is the volume fraction of the porosity. The material properties of a perfect FG plate can be obtained when the volume fraction of porosity β is set to zero.

3 Kinematic, strain and stress relations

The assumed displacement field can be defined by [11]

$$\begin{aligned} U(x, y, z, t) &= u_0(x, y, t) - z \frac{\partial w_b}{\partial x} - f(z) \frac{\partial w_s}{\partial x} \\ V(x, y, z, t) &= v_0(x, y, t) - z \frac{\partial w_b}{\partial y} - f(z) \frac{\partial w_s}{\partial y} \\ W(x, y, z, t) &= w_b(x, y, t) + w_s(x, y, t) \end{aligned} \quad (6)$$

Also, $f(z)$ refers to the variation of the transverse shear strain along with the plate thickness. In this study, we have taken it as

$$f(z) = z - \frac{h}{\pi} \sin \left(\frac{\pi z}{h} \right) \quad (7)$$

The linear constitutive relations of an FG plate can be written as

$$\begin{Bmatrix} \sigma_x \\ \sigma_y \\ \tau_{xy} \end{Bmatrix} = \begin{bmatrix} C_{11} & C_{12} & 0 \\ C_{12} & C_{22} & 0 \\ 0 & 0 & C_{66} \end{bmatrix} \begin{Bmatrix} \varepsilon_x \\ \varepsilon_y \\ \gamma_{xy} \end{Bmatrix}, \quad \begin{Bmatrix} \tau_{yz} \\ \tau_{zx} \end{Bmatrix} = \begin{bmatrix} C_{44} & 0 \\ 0 & C_{55} \end{bmatrix} \begin{Bmatrix} \gamma_{yz} \\ \gamma_{zx} \end{Bmatrix} \quad (8)$$

$$\begin{aligned} C_{11} &= C_{22} = \frac{E(z)}{1-\nu^2} \\ C_{12} &= \frac{\nu E(z)}{1-\nu^2} \\ C_{44} &= C_{55} = C_{66} = \frac{E(z)}{2(1+\nu)} \end{aligned} \quad (9)$$

4 Equations of motion

Hamilton's principle is herein utilized to determine the equations of motion [12]:

$$0 = \int_0^t (\delta U - \delta K) dt, \quad (10)$$

where δU is the variation of strain energy and δK is the variation of kinetic energy. The equations of motion can be expressed in terms of displacements (u_0 , v_0 , w_b , w_s) and the appropriate equations take the form:

$$\begin{aligned} A_{11} \frac{\partial^2 u_0}{\partial x^2} + A_{66} \frac{\partial^2 u_0}{\partial y^2} + (A_{12} + A_{66}) \frac{\partial^2 v_0}{\partial x \partial y} - B_{11} \frac{\partial^3 w_b}{\partial x^3} - (B_{12} + 2B_{66}) \frac{\partial^3 w_b}{\partial x \partial y^2} \\ - B_{11}^s \frac{\partial^3 w_s}{\partial x^3} - (B_{12}^s + 2B_{66}^s) \frac{\partial^3 w_s}{\partial x \partial y^2} = I_0 \ddot{u}_0 - I_1 \frac{\partial \ddot{w}_b}{\partial x} - J_1 \frac{\partial \ddot{w}_s}{\partial x}, \end{aligned} \quad (11)$$

$$\begin{aligned} (A_{12} + A_{66}) \frac{\partial^2 u_0}{\partial x \partial y} + A_{66} \frac{\partial^2 v_0}{\partial x^2} + A_{22} \frac{\partial^2 v_0}{\partial y^2} - (B_{12} + 2B_{66}) \frac{\partial^3 w_b}{\partial x^2 \partial y} - B_{22} \frac{\partial^3 w_b}{\partial y^3} \\ - B_{22}^s \frac{\partial^3 w_s}{\partial y^3} - (B_{12}^s + 2B_{66}^s) \frac{\partial^3 w_s}{\partial x^2 \partial y} = I_0 \ddot{v}_0 - I_1 \frac{\partial \ddot{w}_b}{\partial y} - J_1 \frac{\partial \ddot{w}_s}{\partial y} \end{aligned} \quad (12)$$

$$\begin{aligned}
& B_{11} \frac{\partial^3 u_0}{\partial x^3} + (B_{12} + 2B_{66}) \frac{\partial^3 u_0}{\partial x \partial y^2} + (B_{12} + 2B_{66}) \frac{\partial^3 v_0}{\partial x^2 \partial y} + B_{22} \frac{\partial^3 v_0}{\partial y^3} - D_{11} \frac{\partial^4 w_b}{\partial x^4} \\
& - 2(D_{12} + 2D_{66}) \frac{\partial^4 w_b}{\partial x^2 \partial y^2} - D_{22} \frac{\partial^4 w_b}{\partial y^4} - D_{11}^s \frac{\partial^4 w_s}{\partial x^4} - 2(D_{12}^s + 2D_{66}^s) \frac{\partial^4 w_s}{\partial x^2 \partial y^2} \quad (13) \\
& - D_{22}^s \frac{\partial^4 w_s}{\partial y^4} = I_0 (\ddot{w}_b + \ddot{w}_s) + I_1 \left(\frac{\partial \ddot{u}_0}{\partial x} + \frac{\partial \ddot{v}_0}{\partial y} \right) - I_2 \nabla^2 \ddot{w}_b - J_2 \nabla^2 \ddot{w}_s,
\end{aligned}$$

$$\begin{aligned}
& B_{11}^s \frac{\partial^3 u}{\partial x^3} + (B_{12}^s + 2B_{66}^s) \frac{\partial^3 u}{\partial x \partial y^2} + (B_{12}^s + 2B_{66}^s) \frac{\partial^3 v}{\partial x^2 \partial y} + B_{22}^s \frac{\partial^3 v}{\partial y^3} - D_{11}^s \frac{\partial^4 w_b}{\partial x^4} \\
& - 2(D_{12}^s + 2D_{66}^s) \frac{\partial^4 w_b}{\partial x^2 \partial y^2} - D_{22}^s \frac{\partial^4 w_b}{\partial y^4} - H_{11}^s \frac{\partial^4 w_s}{\partial x^4} - 2(H_{12}^s + 2H_{66}^s) \frac{\partial^4 w_s}{\partial x^2 \partial y^2} \quad (14) \\
& - H_{22}^s \frac{\partial^4 w_s}{\partial y^4} + A_{55}^s \frac{\partial^2 w_s}{\partial x^2} + A_{44}^s \frac{\partial^2 w_s}{\partial y^2} = I_0 (\ddot{w}_b + \ddot{w}_s) + J_1 \left(\frac{\partial \ddot{u}_0}{\partial x} + \frac{\partial \ddot{v}_0}{\partial y} \right) - J_2 \nabla^2 \ddot{w}_b - K_2 \nabla^2 \ddot{w}_s
\end{aligned}$$

5 Navier solution for simply supported rectangular plates

The Navier solution method is utilized to calculate the analytical solutions in which the displacement variables are expressed as the product of arbitrary parameters and known trigonometric functions in order to satisfy the equations of motion and boundary conditions.

$$\begin{Bmatrix} u_0 \\ v_0 \\ w_b \\ w_s \end{Bmatrix} = \sum_{m=1}^{\infty} \sum_{n=1}^{\infty} \begin{Bmatrix} U_{mn} e^{i\omega t} \cos(\lambda x) \sin(\mu y) \\ V_{mn} e^{i\omega t} \sin(\lambda x) \cos(\mu y) \\ W_{bmn} e^{i\omega t} \sin(\lambda x) \sin(\mu y) \\ W_{smn} e^{i\omega t} \sin(\lambda x) \sin(\mu y) \end{Bmatrix}, \quad (15)$$

where U_{mn} , V_{mn} , W_{bmn} , and W_{smn} , are arbitrary parameters and $\omega = \omega_{mn}$ denotes the eigenfrequency associated with the $(m, n)^{\text{th}}$ eigenmode. Substituting the expression of Eq. (15) into the governing equations (11)-(14), then integrating over the domain of solution, after some mathematical manipulations, one may reach the following equations:

$$\begin{bmatrix} S_{11} & S_{12} & S_{13} & S_{14} \\ S_{12} & S_{22} & S_{23} & S_{24} \\ S_{13} & S_{23} & S_{33} & S_{34} \\ S_{14} & S_{24} & S_{34} & S_{44} \end{bmatrix} - \omega^2 \begin{bmatrix} m_{11} & 0 & 0 & 0 \\ 0 & m_{22} & 0 & 0 \\ 0 & 0 & m_{33} & m_{34} \\ 0 & 0 & m_{34} & m_{44} \end{bmatrix} \begin{Bmatrix} U_{mn} \\ V_{mn} \\ W_{bmn} \\ W_{smn} \end{Bmatrix} = \begin{Bmatrix} 0 \\ 0 \\ 0 \\ 0 \end{Bmatrix} \quad (16)$$

6 Numerical Results and discussion

This section presents the numerical results for free vibration of FG plates. The effect of the distribution pattern of porosity and the plate's geometrical properties is studied. The FG plates are made of Aluminum (Al) as metal part and Aluminum oxide (Al_2O_3) as ceramic part. The material properties of the FG plate used in this study are given in Table 1 [9].

Table 1. Material properties of metal and ceramic.

Material	Young's modulus (GPa)	Mass density (kg/m^3)	Poisson's ratio
Aluminum (Al)	70	2702	0.3
Aluminum oxide (Al_2O_3)	380	3800	0.3

Several numerical examples are presented to verify the accuracy of the present solution and investigate the effects of the power-law index, length-to-thickness ratio, porosity distributions pattern, and the porosity parameters on the natural frequencies of FG porous plates. For convenience, the following non-dimensional parameter is used:

$$\bar{\omega} = \frac{\omega a^2}{h} \sqrt{\frac{\rho_c}{E_c}} \quad (17)$$

First, the accuracy of the presented solution is investigated. To this end, in Table 2, the variation of the natural frequency of porous simply supported FG plate for different values of a/h , β and porosity distribution pattern are presented. Results of the classical plate theory (CPT) are also included for comparison purposes. The results show that increasing porosity leads to a decrease in the natural frequency. Moreover, as the plate becomes thicker, the difference between the CPT and present solution increases. However, CPT and the present solution results show a good agreement for thin plates. It is worth mentioning that the CPT results are obtained by setting $f(z)=0$ in Eq. (6).

Table 2. Effects of distribution shape of the porosity on the nondimensional fundamental frequency ($\bar{\omega}$) of simply supported Al/Al₂O₃ square plates, $k=1$.

a/h	Theory	β	Distribution shape of the porosity			
			Uniform	X	O	V
5	CPT	0	4.4048	4.4048	4.4048	4.4048
		0.1	4.3040	4.5137	4.4240	4.4222
		0.2	4.1595	4.6043	4.4425	4.4410
	Present	0	4.0784	4.0784	4.0784	4.0784
		0.1	3.9984	4.1644	4.0896	4.0924
		0.2	3.8823	4.2351	4.0994	4.1076
10	CPT	0	4.5194	4.5194	4.5194	4.5194
		0.1	4.4179	4.6319	4.5428	4.5388
		0.2	4.2723	4.7251	4.5659	4.5597
	Present	0	4.4193	4.4193	4.4193	4.4193
		0.1	4.3244	4.5244	4.4397	4.4374
		0.2	4.1875	4.6111	4.4595	4.4569
20	CPT	0	4.5493	4.5493	4.5493	4.5493
		0.1	4.4477	4.6629	4.5738	4.5692
		0.2	4.3018	4.7567	4.5982	4.5907
	Present	0	4.5228	4.5228	4.5228	4.5228
		0.1	4.4229	4.6344	4.5465	4.5424
		0.2	4.2793	4.7264	4.5699	4.5634

Fig. 2 shows the effect of the length-to-thickness ratio on the non-dimensional natural frequency of square Al/Al₂O₃ FG plates with different porosity distribution patterns. The results show that the X shape porosity distribution has the highest natural frequency while the homogenous (uniform) porosity distributions has the lowest one.

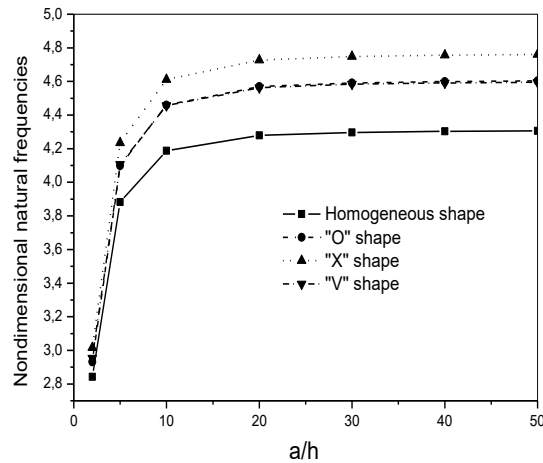


Fig. 2. Effect of length-to-thickness on the dimensionless fundamental frequency of Al/Al₂O₃ FG square plate ($k=1$ and $\beta=0.2$).

7 Conclusions

This study focused on the impact of the distribution pattern of porosity on the free vibration of FG porous plates. Trigonometric shear deformation theory was employed for this purpose. Four types of porosity distribution were considered. The study examined the effects of porosity, porosity distribution pattern, FGM distribution parameter, and plate geometrical parameters such as length-to-thickness ratio on the free vibration of FG plates. The accuracy of the presented analytical solution was confirmed by comparing the results with existing data in the literature. Additionally, the results indicated that the X-shaped porosity distribution had the highest natural frequency, while the homogeneous distribution of porosities had the lowest.

References

- [1] Niknam, H., A. Fallah, and M.M. Aghdam, *Nonlinear bending of functionally graded tapered beams subjected to thermal and mechanical loading*. International Journal of Non-Linear Mechanics, 2014. **65**: p. 141-147 DOI: <https://doi.org/10.1016/j.ijnonlinmec.2014.05.011>.
- [2] Hadji, L., V. Plevris, and G. Papazafeiropoulos, *Investigation of the Static Bending Response of FGM Sandwich Plates*. Journal of Applied and Computational Mechanics, 2023: p. - DOI: <https://doi.org/10.22055/jacm.2023.44278.4194>.
- [3] Shahsavari, D., M. Shahsavari, L. Li, and B. Karami, *A novel quasi-3D hyperbolic theory for free vibration of FG plates with porosities resting on Winkler/Pasternak/Kerr foundation*. Aerospace Science and Technology, 2018. **72**: p. 134-149 DOI: <https://doi.org/10.1016/j.ast.2017.11.004>.
- [4] Zhu, J., Z. Lai, Z. Yin, J. Jeon, and S. Lee, *Fabrication of ZrO₂-NiCr functionally graded material by powder metallurgy*. Materials Chemistry and Physics, 2001. **68**(1): p. 130-135 DOI: [https://doi.org/10.1016/S0254-0584\(00\)00355-2](https://doi.org/10.1016/S0254-0584(00)00355-2).

- [5] Wattanasakulpong, N., B. Gangadhara Prusty, D.W. Kelly, and M. Hoffman, *Free vibration analysis of layered functionally graded beams with experimental validation*. *Materials & Design* (1980-2015), 2012. **36**: p. 182-190 DOI: <https://doi.org/10.1016/j.matdes.2011.10.049>.
- [6] Wattanasakulpong, N. and V. Ungbhakorn, *Linear and nonlinear vibration analysis of elastically restrained ends FGM beams with porosities*. *Aerospace Science and Technology*, 2014. **32**(1): p. 111-120 DOI: <https://doi.org/10.1016/j.ast.2013.12.002>.
- [7] Hadji, L., V. Plevris, and R. Madan. *A Static and Free Vibration Analysis of Porous Functionally Graded Beams*. in *Proceedings of the 2nd International Conference on Civil Infrastructure and Construction (CIC 2023)*. 2023. Doha, Qatar: QU Press. p. 433-441. DOI: <https://doi.org/10.29117/cic.2023.0059>.
- [8] Hadji, L., V. Plevris, and R. Madan, *Investigating the Impact of Porosity Distribution and Grading Parameter on the Free Vibration of Functionally Graded Beams*, in *9th ECCOMAS Thematic Conference on Computational Methods in Structural Dynamics and Earthquake Engineering (COMPdyn 2023)*. 2023: Athens, Greece.
- [9] Thai, H.-T., T.-K. Nguyen, T.P. Vo, and J. Lee, *Analysis of functionally graded sandwich plates using a new first-order shear deformation theory*. *European Journal of Mechanics - A/Solids*, 2014. **45**: p. 211-225 DOI: <https://doi.org/10.1016/j.euromechsol.2013.12.008>.
- [10] Hadj, B., B. Rabia, and T.H. Daouadji, *Influence of the distribution shape of porosity on the bending FGM new plate model resting on elastic foundations*. *Structural Engineering and Mechanics*, 2019. **72**(1): p. 61-70 DOI: <https://doi.org/10.12989/sem.2019.72.1.061>.
- [11] Hadji, L., H.A. Atmane, A. Tounsi, I. Mechab, and E.A. Adda Bedia, *Free vibration of functionally graded sandwich plates using four-variable refined plate theory*. *Applied Mathematics and Mechanics*, 2011. **32**(7): p. 925-942 DOI: <https://doi.org/10.1007/s10483-011-1470-9>.
- [12] Reddy, J.N., *Energy Principles and Variational Methods in Applied Mechanics*. 3rd ed. 2017: Wiley, ISBN: 978-1-119-08737-3.